2024 10th International Conference on Control, Decision and Information Technologies
CoDIT 2024 | Valletta, Malta / July 01-04, 2024 Technically co-sponsored by IEEE & IFAC

2024 10th International Conference on Control, Decision and Information Technologies (CoDIT) | 979-8-3503-7397-4/24/$31.00 ©2024 IEEE | DOI: 10.1109/CoDIT62066.2024.10708474

Sliding mode controller for re-entry dynamics of spacecraft reusable type Starship*

Jose Luis Huayanay Villar[1], Cristhian Aldana[1], Wilmer Moncada[2], Edwin Saavedra[1] and Yesenia Saavedra[1]

***Abstract*— The behavior of a reusable Starship spacecraft during re-entry into Earth's upper atmosphere is governed by aerodynamic principles. This study aims to develop a sliding mode controller by constructing a nonlinear dynamic model with three degrees of freedom, considering external perturbations. The methodology involves applying a sliding mode control law to manage vibrations due to air friction, impact pressure on the spacecraft's front surface, and lateral friction. Simulation results demonstrate that the initial approximation of the spacecraft's reference and control trajectory achieves stable control behavior and safe re-entry. The controller's reliability and the stability of the closed-loop system are significantly enhanced, though transient responses vary due to the nonlinearity of re-entry dynamics.**

I. Introduction

This atmosphere re-entry , is defined as the trajectory described by the spacecraft from the last orbit or suborbital to the lower layers of the Earth's atmosphere, and overcome a large amount of uncertainty, outside interference, and complex route constraints [1]. There are different types of re-entries such as ballistics and Elevation, some controlled and some uncontrolled. In the case of aerodynamically controlled reentry, the main requirement is that the spacecraft have a high L/D ratio greater than the value 1.0 [2]. Next, the focus for this work will be mainly on analyzing the dynamic and control models to model the controlled re-entry, of reusable spacecraft (RS) [3], with configuration, winged/lifting bodies (WLB) or spacecraft. "These reusable spacecraft are is defined as a vehicle with an excess lift-to-drag (L/D) ratio 1.0 at speeds supersonic (above 5 times the speed of sound) and greater than 4.0 at subsonic speeds, in combination with high controllability" [2], [4]. During the re-entry phase, the vehicle's altitude and speed will vary rapidly and dramatically as an RS go through a series of flight envelopes[5]. "At the same time, they suffered from poor flying conditions, uncertainty of main parameter and unknown external noise" [6]. Vinh NX. and Busemann [7] "presented studies of atmospheric reentry flight mechanics in light of its importance to the space shuttle, based on Loh's second-order theory for reentry trajectories which is presented together with the classical theories of Yaroshevskii and Chapman" [8]. Such spacecraft require effective flight control planning and control precision to improve operational reliability. "Sliding mode control (SMC) is also used to design flight control systems that can operate with limited thrust and cause significant damage to the frame or actuator, e.g. steering motion"[9]. Bailing Tian and Qun Zong already in 2013 present a design of sliding mode controllers (SMC) [10], [11], [12] of semi-continuous advanced for the boosters can be reused upon re-entry of the x-33 which demonstrates Effectiveness of the proposed control strategy in future guidance and providing a safe and stable return flight [13]. PM Tiwari, S Janardhanan in [14] "Adaptive, challenging terminal, fast travel mode, rigid spacecraft attitude control". These authors develop a robust finite-time adaptive SMC method that is it has been Proposed attitude control of a rigid spacecraft. The control method was obtained using a new one fast slip surface terminal with the right range. In the work of Yao Zhang and Shengjing Tang [15] Based on the non-singulars, fast terminal SMC Quick algorithm of super -superficial and adaptable super twist, new integration law related to sliding control with the last time of relationships that can be achieved for reusing vehicles to start the use. Later Shtisel, JD McSuffie developed sliding mode for X-33 vehicle for atmospheric applications to re-enter again [16].

At the same time, authors such as Cantou [17] are studying actuators for Starchip Spacex (BFS), indicates that the wing is not designed forlow-speed and subsonic flight [18]. However, in conditions of supersonic flow after entering the atmosphere, such wings are quite effective. "For BFS, the L/D ratio can range from 1.35 to over 2.0, which is normal due to the relatively small wing size" [19]. Therefore, int the present work the SMC This method is considered one of the most promising and reliable control technologies. Under appropriate conditions, it is insensitive to various changes in parameters and external influences, thanks to which it is characterized by a fast dynamic response, making it a good potential method for flight control systems [20]. This document presents, the correct functioning of the system by following these steps:

- In the first stage, analysis of the forces on an orbiting spacecraft in Section II, Subsection II-A, Subsection II-B.
- The 3DOFF reentry mathematical model assuming a spacecraft reusable is modeled by differential equations (ODE) in Section III, Subsection III-A highlight the

*The National Institute for Space Research (INPE-Brazil)/Cnpq. The Institute for Research in Economics and Productive Efficiency of the National University of Frontera (INDEEP-UNF) and UDEC.

[1]J. L. H. Villar, C. Aldana, E. Saavedra, Y. saavedra, with Universidad Nacional de Frontera (UNF), Sullana, Perú. E-mail: jhuayanav@unf.edu.pe, jose.villar@inpe.br, caldana@unf.edu.pe, edsaana@icloud.com and ysaavedra@unf.edu.pe.

[2] W. Moncada with Universidad Nacional de San Cristóbal de Huamanga (UNSCH), E-mail: wilmer.moncada@unsch.edu.pe.

nonlinear dynamics, initial conditions and parameters.
- In this step Section IV Reentry dynamics sliding mode control

II. Forces on an orbiting spacecraft

The RS and the planet are assumed to be in relative motion of two bodies. For a spherical planet,the g (m/s^2) gravitational acceleration :

$$g = \frac{\mu}{r^2} \tag{1}$$

where parameter in particular $\mu = 3.9859383624 \times 10^{14}$ (m^3/s^2), with:

$$r = R_e + h \tag{2}$$

r (m) radio Distance from the center or origin of the planet [21], R_e (m) is the radius of earth with h (m) altitude.

A. Drag forces

According to [22] the mathematical definition of the aerodynamic force opposing the motion of the spacecraft v (m/s) wind speed, is known as drag (D)

$$D = \frac{SC_D\rho v^2}{2} \tag{3}$$

Where is proportional to the body's reference surface S (m^2), generally taken equal to the wing surface for a space shuttle wing, and which depends on the drag coefficient C_D

$$C_D(\alpha) = a_0 + a_1(\alpha) + a_2(\alpha)^2 \tag{4}$$

a_0, a_1 and a_2, constant parameters, the coefficients can also depend on the angle of attack α (rad) (AOA). So ρ (kg/m^3) is the atmospheric density that varies with attitude and water vapor saturation. Density in Isothermal Atmosphere [23], [7]

$$\rho_i = \rho_0.e^{-(r-R_e)/hr)} \tag{5}$$

The temperature T is uniform regardless of altitude. With every increase in altitude by h_r(m), the pressure decreases by a factor. For this environment model, that is approximately 8.41 km at a $T = 16$ °C, $e = 2.73$. Density in Adiabatic Atmosphere [24]

$$\rho_a = \rho_0\left(1 - \frac{h}{h_0}\right)^{\frac{1}{\kappa-1}} \longrightarrow h_0 = \frac{\kappa p_0}{(\kappa-1)\rho_0 g} \tag{6}$$

k the adiabatic exponent of dry air, g the acceleration of gravity, ρ_0 relative density, P_0 relative pressure (bar).

B. Lifting force

Another component of aerodynamic force is the spacecraft's relative velocity perpendicular to the atmosphere is known as lift (L), we have:

$$L = \frac{SC_L\rho v^2}{2} \tag{7}$$

C_L lift coefficient [22]

$$C_L(\alpha) = b_0 + b_1(\alpha) \tag{8}$$

where b_0 and b_1 , are constant parameters.

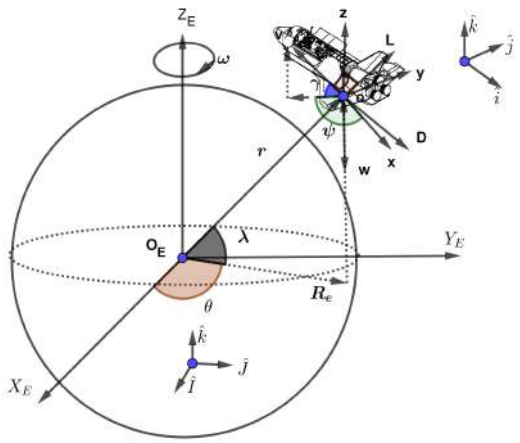

Fig. 1. For fixed planet (O_E) and local horizon frames, for flight atmospheric spacecraft Reusable in (0) (developed in Geogebra)

III. Re-entry mathematical model

In this first section, consider how one traveling in the spacecraft makes a reentry into the Earth's atmosphere [21],[25]. Assuming the earth is a stationary $(0_E, X_E, Y_E, Z_E)$ reference point, and deciding ignoring the Earth's orbital motion around the Sun, assumes for limited studies of flight relative to Earth. Then assume the frame $(0_E, X_E, Y_E, Z_E)$ is fixed. considered the unit vectors $\hat{I}$, $\hat{J}$, $\hat{K}$ along the axes O_EX_E, O_EY_E and O_EZ_E, respectively. In a stationary frame of reference, they are represented by two angles, longitude λ, and latitude θ, see Figure 1. Angular velocity of the Earth relative to a fixed plane O_EZ_E is then ω. Next, we will choose the orientation of the spaceship (o,x,y,z) at a position of $r = R_e + h$ from Earth or it could be considered a orig point, ox is on the direction south, oy is east, and axes oz is vertically ; the unit vectors $\hat{i}$, $\hat{j}$, $\hat{k}$ whit represent the directions of axes ox, oy and oz, respectively [26, Eq.29-34]. Likewise, the relative speed of the spacecraft reusable will be used v (m/s), flight path angle γ (rad) , whit azimuth ψ (rad) . Considered in the present work reentry spacecraft, for 3DOFF translations dynamics develop-eds in [27, Pag. 6], [10, Eq. 1-6], [28, Eq. 33], [7, Eq. 14], [29], [2] governed by the following nonlinear differential equations:

A. Transnational Reentry Equation

$$\dot{h} = \dot{r} = \sin(\gamma).v, \tag{9}$$

$$\dot{\lambda} = \frac{v}{r.\cos(\theta)}.\cos(\gamma).\sin(\psi), \tag{10}$$

$$\dot{\theta} = \frac{v}{r}.\cos(\gamma).\cos(\phi), \tag{11}$$

$$\begin{aligned}\dot{v} = -\frac{D}{m} - g\sin(\gamma) + \omega^2 r\cos^2(\theta)\sin(\gamma) - \\ \omega^2\cos(\gamma).\sin(\theta).\cos(\psi)\cos(\theta),\end{aligned} \tag{12}$$

$$\dot{\gamma} = \frac{L}{v}\cos(\sigma) + (\frac{v}{r} - \frac{g}{v})\cos(\gamma) + \frac{\omega^2}{v} r\cos(\theta)[\sin(\gamma)\cos(\psi)\sin(\theta) + \cos(\gamma).\cos(\theta)] + 2.\sin(\psi).\omega.\cos(\theta), \quad (13)$$

$$\dot{\psi} = \frac{v}{r}.\cos(\gamma)\sin(\psi)\tan(\theta) + \frac{L}{mv\cos(\gamma)}\sin(\sigma) + \frac{\omega^2}{v\cos(\gamma)} r\sin(\psi)\sin(\theta).\cos(\theta) + 2\omega(\sin(\theta) - \tan(\gamma).\cos(\psi).\cos(\theta)). \quad (14)$$

Where m (kg) is mass spacecraft, ω represents Earth's angular velocity, g (m/s^2) gravitational acceleration, σ is bank angle. Then we will propose that a technique that stabilizes reentry flight so that the spacecraft can fly steadily in the atmosphere for a long time, figure (2) and figure (3). In this first step, if we neglect the Earth's rotation, $\omega = 0$, we can rewrite the equations (9) to (14) to the simplified dynamics model [22], [26]:

$$\dot{r} = \sin(\gamma).v, \quad (15)$$

$$\dot{\lambda} = \frac{v}{\cos(\theta).r}.\cos(\gamma).\sin(\psi), \quad (16)$$

$$\dot{\theta} = \frac{v}{r}.\cos(\gamma).\cos(\phi), \quad (17)$$

$$\dot{v} = -g.\sin(\gamma) - \frac{D}{m}, \quad (18)$$

$$\dot{\gamma} = \frac{L}{v}.\cos(\sigma) + \cos(\gamma).(\frac{v}{r} - \frac{g}{v}), \quad (19)$$

$$\dot{\psi} = \frac{v}{r}.\cos(\gamma).\tan(\theta).\sin(\psi) + \sin(\sigma).\frac{L}{m.v.\cos(\gamma)}. \quad (20)$$

An option that could be considered control input is the bank angle σ. "The applied method is based on the quasi-equilibrium sliding condition defined by the expression" [2]:

$$L\sin(\sigma) + (g - \frac{v^2}{r})m = 0 \quad (21)$$

TABLE I
DATABASE FOR SIMULATION [17],[30]

Nome	Spacecraft reusable type Starship
Mass m (kg)	7169.6
Area (S) m^2	240.0
$\rho_0(kg/m^3)$	1,225
R_e(m)	6371203,92
$\mu(km^3/s^2)$	3.9800×10^{14}
T (s)	86164.09054
h_r (m)	7143
ω (rad/s)	7.292×10^{-5}

For the preliminary bank-angle, control law:

$$\sigma = \arcsin(\frac{m}{L}(g - \frac{v^2}{r})) \quad (22)$$

substituting the equation 1 in 22 and derived, we get

$$\dot{\sigma} = -\frac{4\mu m(v+r)}{C_L\rho v^3\sqrt{1-(\frac{m}{L}(g-\frac{v^2}{r}))^2 r^3}} + \frac{2m}{\rho\sqrt{1-(\frac{m}{L}(g-\frac{v^2}{r}))^2 r^2}} \quad (23)$$

Note that in the figure 2 with data Tab. I the orbital states change smoothly for all seems to have satisfied the path constraints and then integrated the translational command belong to dynamic equation in the absence of uncertainty, the same gives a nominal orbital profile.

IV. REENTRY DYNAMICS SLIDING MODE CONTROL

This means that the following equations hold:

$$\lim_{t \Longrightarrow \infty} \|\sigma_{ref} - \sigma\| = 0 \quad (24)$$

where σ_{ref} is guidance groups are created on the basis of guidance and reference signal. system define the sliding mode variable [31, eq.27]

$$s = \sigma_{ref} - \sigma \quad (25)$$

then $s = 0$ describes the expected dynamics of the system. Then the task of the controller is to ensure that the trajectory of the system reach an arbitrarily small neighborhood of the origin in a finite time and stay there despite the uncertainty. the variable structure control law was chosen [32, eq.19]

$$u(t) := \begin{cases} u^-(t), & \text{is } s < 0, \\ u^+(t), & \text{is } s > 0 \end{cases} \quad (26)$$

in which

$$u^+(t) = \overline{d}(t) + \delta \quad (27)$$

Is a control modulation signal, possibly extreme such as the *flaps our wing body on*

$$u^-(t) = \underline{d}(t) - \delta \quad (28)$$

is another control modulation signal, possibly extreme such as the actuator containing surface deflections aerodynamics *flaps our wing body off*, e for arbitrary constant $0 < \delta < u(t) + d(t)$ well enough. whit disturbances upper limit $\overline{d}(t) \in \mathbb{R}$ and the disturbances lower limit $\underline{d}(t) \in \mathbb{R}$ are the continuous signal of the parts that know how to satisfy the uneven [32]:

$$\underline{d}(t) \leq d(t) \leq \overline{d}(t), \quad \forall t \geq 0, \quad (29)$$

in which $d(t) \in \mathbb{R}$ the noise signal is removed by the controller. During turbulence, one of the main problems of sliding control is solved: chattering (air friction), the impact pressure on the spacecraft side breaking through, or Drag due to side friction. Deriving the equation 25 and using the equation 39, The driving force of the sliding mode is defined as

$$\dot{s} = \dot{\sigma}_{ref} - \dot{\sigma} = \frac{1}{r^3}(\dot{\sigma}_{ref} + \frac{4\mu m(v+r)}{C_L\rho v^3\sqrt{1-(\frac{m}{L}(g-\frac{v^2}{r}))^2}}) - \frac{1}{r^2}(\frac{2m}{\rho\sqrt{1-(\frac{m}{L}(g-\frac{v^2}{r}))^2}}) \quad (30)$$

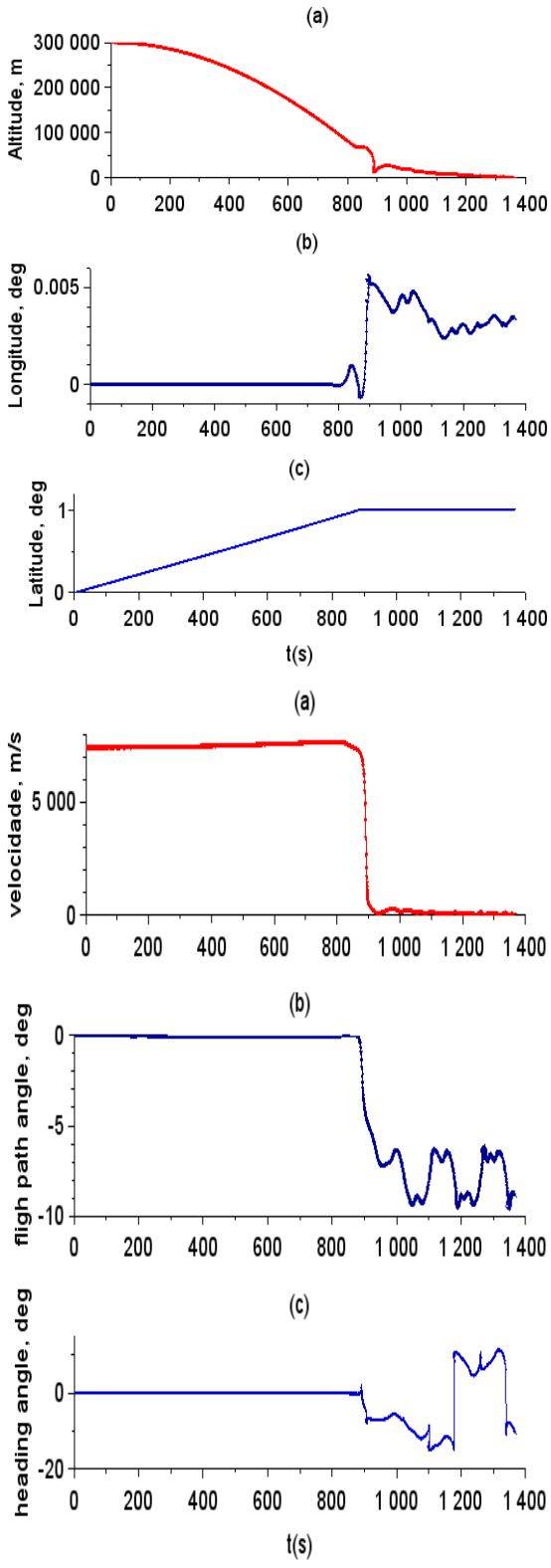

Fig. 2. Solution re-entry trajectories, abscissa is the time in seconds spacecraft reusable type Starship **(a)** state for altitude, **(b)** latitude, **(c)** longitude, **(a)** velocity, **(b)** flight path e **(c)** heading (developed in Scilab)

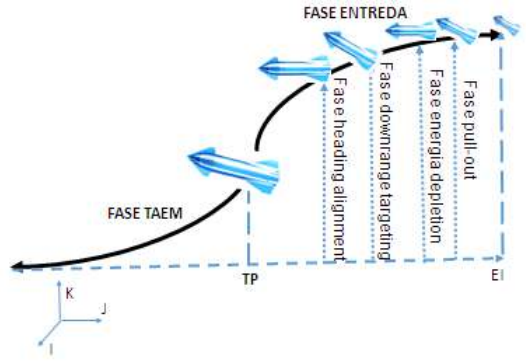

Fig. 3. Fixed planet (O_E) and local horizon frames for atmospheric spacecraft flight in (0)

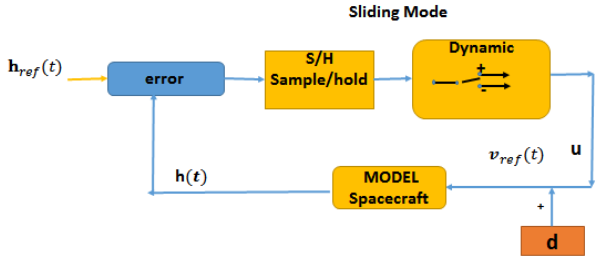

Fig. 4. block diagram design of the proposed controller.

for $r > 0$ is true , then

$$\dot{s} = \frac{2}{r^3} < \frac{2}{r^2} \quad \Longrightarrow \quad \frac{2}{r^3}\frac{\mu(v+r)}{C_L v^3} < \frac{2}{r^2}, \qquad if \quad \mu > 0,\ C_L > 0,\ v > 0 \tag{31}$$

therefore it converges to

$$\dot{s} = \frac{2}{r^3}\frac{\mu(v+r)}{C_L v^3}\left(\frac{2m}{\rho\sqrt{1-(\frac{m}{L}(g-\frac{v^2}{r}))^2}}\right) < \frac{1}{r^2}\left(\frac{2m}{\rho\sqrt{1-(\frac{m}{L}(g-\frac{v^2}{r}))^2}}\right) \quad \Longrightarrow \quad \dot{s} < 0 \tag{32}$$

Therefore it can be concluded that the control takes place in sliding mode s and the differential $\dot{s}$ converge the equilibrium point in a finite time.

A. Analysis stability and robustness

Since rotational motion is much faster than translational motion, the time derivatives of position and velocity are considered negligible for rotational motion, leads to the following system of equations.

$$\dot{\alpha} = -p_x\cos(\alpha)\tan(\beta) - r_z\sin(\alpha)\tan(\beta) + q_y + d_\alpha, \tag{33}$$

$$\dot{\beta} = p_x\sin(\alpha) + r_z\cos(\alpha) + d_\beta, \tag{34}$$

$$\dot{\sigma} = -p_x\cos(\alpha)\cos(\beta) - q_y\sin(\beta) - r_z\sin(\alpha)\cos(\beta) + d_\sigma \tag{35}$$

and angular rates of the reference frame (fixed body).

$$\dot{p}_x = \frac{M_x}{I_x} + \frac{(I_y - I_z)}{I_x}q_y r_z \tag{36}$$

$$\dot{q}_y = \frac{M_y}{I_y} + \frac{(I_z - I_x)}{I_y} p_x r_z \tag{37}$$

$$\dot{r}_z = \frac{M_z}{I_{zz}} + \frac{(I_x - I_y)}{I_z} p_x q_y \tag{38}$$

New equation of rotation shown in the equations (33) to (35), for the control-oriented model, is expressed in the form below:

$$I\dot{W} = -\omega^x I W + M + \Delta D \tag{39}$$

$$\dot{\Theta} = A_2(\Theta, T) + R(\Theta)W + d \tag{40}$$

$$T = \begin{bmatrix} h \\ \lambda \\ \theta \end{bmatrix}, \quad x_1 = \begin{bmatrix} v \\ \gamma \\ \psi \end{bmatrix}, \quad \Theta = \begin{bmatrix} \alpha \\ \beta \\ \sigma \end{bmatrix}, \quad W = \begin{bmatrix} p_x \\ q_y \\ r_z \end{bmatrix} \tag{41}$$

$$M = \begin{bmatrix} m_x \\ m_y \\ m_z \end{bmatrix}, \quad d = \begin{bmatrix} d_\alpha \\ d_\beta \\ d_\sigma \end{bmatrix} \quad u = \begin{bmatrix} \delta_x \\ \delta_y \\ \delta_z \end{bmatrix} \tag{42}$$

where d is disturbance, the matrix ω^x is defined as

$$\omega^x = \begin{bmatrix} 0 & -r_z & q_y \\ r_z & 0 & -p_x \\ -q_y & p_x & 0 \end{bmatrix} \tag{43}$$

Torque control $M = [M_x, M_y, M_z]^T$ formed by the airfoils (usually containing the elevators, ailerons, and rudders) and the RCS (reaction control system), expressed by the following equation:

$$M = D_s \delta \tag{44}$$

where D_s is a sensitivity matrix, and $\delta = [\delta_x, \delta_y, \delta_z]^T$ is a drive vector that includes the airfoil deflection and the various RCS engine states.

The tracking error is defined as

$$e_1 = \Theta_r - \Theta = [e_{11}, e_{12}, e_{13}]^T \tag{45}$$

onde $e_{11} = \alpha_r - \alpha$, $e_{12} = \beta_r - \beta$, $e_{13} = \sigma_r - \sigma$

V. Simulation Results

The approximation of the model is done by Sci-lab 6.1.0. and FORTRAN. The proposed controller is basically a very good known driver that suffers from the drawback of Chattering phenomenon Figure (6), and Sigmund function Figure (5). Using a fixed step, the Range-Kutta integral of order 6. In

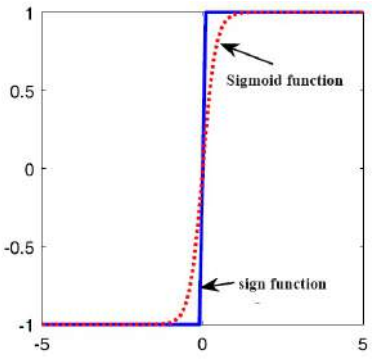

Fig. 5. The sign function and the bipolar Sigmund function

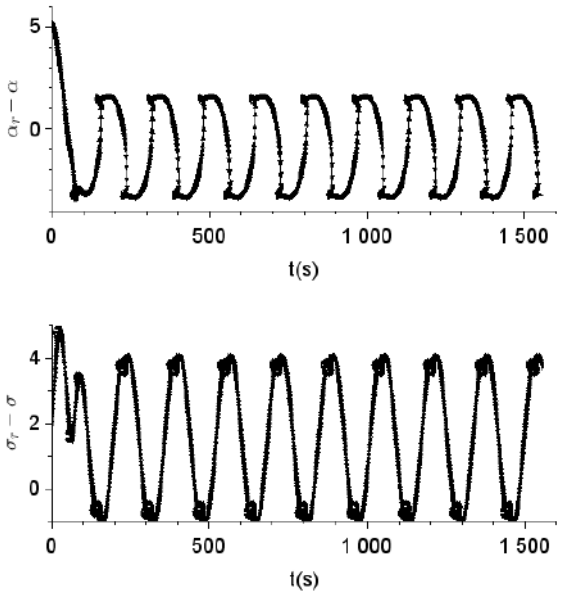

Fig. 6. Error in position tracking and chattering problem

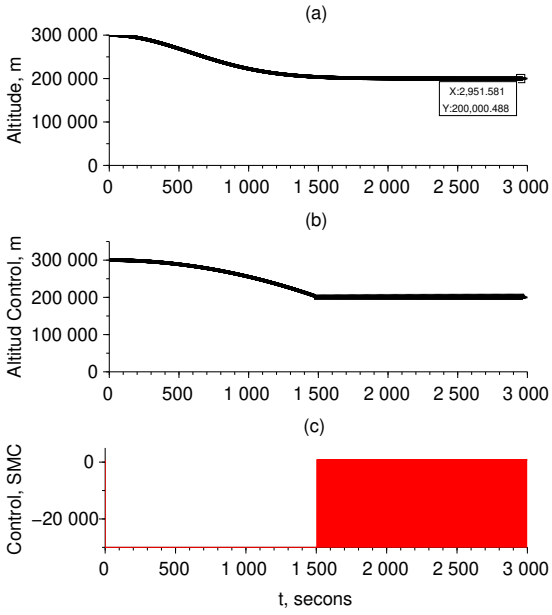

Fig. 7. Illustration for attitude stability spacecraft $h_f = 200000$ m in **(a)** following to **(b)** attitude control and control signal (red) in **(c)** activate at high frequency

Figure (6), reference commands, angle of attack and angle of yaw should only be specified as $\alpha_r = 7, \sigma_r = 3$ It is observed in Figure (7), excellent transient responses of sliding mode control to non-linear dynamics of attitude spacecraft, block 4. The altitude reference for spacecraft reusable $h_f = 200000$ m, is approximate in a finite time $t_s \approx 1500$,s, and as provided by equations 24 and 32, and not exceed the final value and reaching a better stability.

The re-entry stage mainly includes: re-entry stage (EI), on-site energy management stage - TAEM stage (TP), as shown

in the figure (3). The different flight parameters used in the translation and rotation equations are shown in the figure (3).

VI. Conclusion

A nonlinear controller was developed for a reusable spacecraft, ensuring robust tracking and safe reentry for different altitude references despite uncertainties and external perturbations. The controller operates via a switching effect.

In the case of SpaceX's Starship, instead of generating lift, the design aims to create maximum drag by using the vehicle's entire side for aerodynamic braking. The goal is to eliminate speed as quickly as possible.

The Starship can achieve a 90-degree angle of attack, using its wings as air brakes. These wings are designed not to provide lift but to increase drag by adjusting their angle, affecting the amount of drag at both the top and bottom of the vehicle.

Results obtained with the sliding mode controller should be compared with other methods to improve performance. An improved finite-time sliding mode controller supports efficient vibration control without compromising reliability and accuracy.

The reliability of the regulator is enhanced by the sliding mode method. The stability of the closed-loop system was tested and confirmed, although transients vary due to the non-linearity of the reentry dynamics.

Thanks

The National Institute for Space Research (INPE-Brazil)/Cnpq. The Institute for Research in Economics and Productive Efficiency of the National University of Frontera (INDEEP-UNF) and UDEC. Thanks are also due to the Remote Sensing and Renewable Energy Laboratory of the National University of San Cristóbal de Huamanga (LABTELER-UNSCH).

References

[1] Preado and A. F. B. de Almeida, *A Conquista do Espaço do Sputnik a Missão Centenário*. Editora Livraria da Física, 2007.

[2] G. J. Dominguez Calabuig, "Optimum on-board abort guidance based on successive convexification for atmospheric re-entry vehicles," 2020.

[3] A. S. Filatyev, V. Buzuluk, O. Yanova, N. Ryabukha, and A. Petrov, "Advanced aviation technology for reusable launch vehicle improvement," *Acta Astronautica*, vol. 100, pp. 11–21, 2014.

[4] H. W. Stone and W. M. Piland, "21st century space transportation system design approach-hl-20 personnel launch system," *Journal of Spacecraft and Rockets*, vol. 30, no. 5, pp. 521–528, 1993.

[5] Q. Mao, L. Dou, Q. Zong, and Z. Ding, "Attitude controller design for reusable launch vehicles during reentry phase via compound adaptive fuzzy h-infinity control," *Aerospace Science and Technology*, vol. 72, pp. 36–48, 2018.

[6] Z. Wang, Z. Wu, and Y. Du, "Robust adaptive backstepping control for reentry reusable launch vehicles," *Acta Astronautica*, vol. 126, pp. 258–264, 2016.

[7] N. X. Vinh, A. Busemann, and R. D. Culp, "Hypersonic and planetary entry flight mechanics," *NASA Sti/Recon Technical Report A*, vol. 81, p. 16245, 1980.

[8] D. R. Chapman, *An approximate analytical method for studying entry into planetary atmospheres*. US Government Printing Office, 1959.

[9] R. Hess and S. Wells, "Sliding mode control applied to reconfigurable flight control design," *Journal of Guidance, Control, and Dynamics*, vol. 26, no. 3, pp. 452–462, 2003.

[10] B. Tian, Q. Zong, J. Wang, and F. Wang, "Quasi-continuous high-order sliding mode controller design for reusable launch vehicles in reentry phase," *Aerospace science and technology*, vol. 28, no. 1, pp. 198–207, 2013.

[11] V. I. Utkin, "Sliding mode control design principles and applications to electric drives," *IEEE transactions on industrial electronics*, vol. 40, no. 1, pp. 23–36, 1993.

[12] J. Geng, Y. Sheng, and X. Liu, "Finite-time sliding mode attitude control for a reentry vehicle with blended aerodynamic surfaces and a reaction control system," *Chinese Journal of Aeronautics*, vol. 27, no. 4, pp. 964–976, 2014.

[13] Y. Shtessel and C. Hall, "Sliding mode control of the x-33 with an engine failure," in *36th AIAA/ASME/SAE/ASEE Joint Propulsion Conference and Exhibit*, 1997, p. 3883.

[14] P. M. Tiwari, S. Janardhanan, and M. un Nabi, "Rigid spacecraft attitude control using adaptive non-singular fast terminal sliding mode," *Journal of Control, Automation and Electrical Systems*, vol. 26, no. 2, pp. 115–124, 2015.

[15] Y. Zhang, S. Tang, and J. Guo, "Adaptive-gain fast super-twisting sliding mode fault tolerant control for a reusable launch vehicle in reentry phase," *ISA transactions*, vol. 71, pp. 380–390, 2017.

[16] Y. Shtessel, J. McDuffie, M. Jackson, C. Hall, M. Gallaher, D. Krupp, and N. Hendrix, "Sliding mode control of the x-33 vehicle in launch and re-entry modes," in *Guidance, Navigation, and Control Conference and Exhibit*, 1998, p. 4414.

[17] T. Cantou, N. Merlinge, and R. Wuilbercq, "3DoF simulation model and specific aerodynamic control capabilities for a SpaceX's Starship-like atmospheric reentry vehicle," in *EUCASS 2019*, MADRID, Spain, July 2019. [Online]. Available: https://hal.archives-ouvertes.fr/hal-02362037

[18] L. Friedman, "Future tense: Becoming a multi-planet species," *Communications of the ACM*, vol. 59, no. 5, pp. 136–ff, 2016.

[19] M. Sippel, S. Stappert, and A. Koch, "Assessment of multiple mission reusable launch vehicles," *Journal of Space Safety Engineering*, vol. 6, no. 3, pp. 165–180, 2019.

[20] B. Cong, X. Liu, and Z. Chen, "A novel robust control strategy for spacecraft eigenaxis rotations," *IFAC Proceedings Volumes*, vol. 44, no. 1, pp. 2066–2071, 2011.

[21] A. Tewari, *Atmospheric and space flight dynamics*. Springer, 2007.

[22] J. T. Betts, *Practical Methods for Optimal Control and Estimation Using Nonlinear Programming*. SIAM, 2010, vol. 19.

[23] F. Chen, H. Liu, and S. Zhang, "Time-adaptive loosely coupled analysis on fluid–thermal–structural behaviors of hypersonic wing structures under sustained aeroheating," *Aerospace Science and Technology*, vol. 78, pp. 620–636, 2018.

[24] J. Counihan, "Adiabatic atmospheric boundary layers: a review and analysis of data from the period 1880–1972," *Atmospheric Environment (1967)*, vol. 9, no. 10, pp. 871–905, 1975.

[25] G. N. Kumar, M. S. Ahmed, A. Sarkar, and S. Talole, "Reentry trajectory optimization using gradient free algorithms," *IFAC-PapersOnLine*, vol. 51, no. 1, pp. 650–655, 2018.

[26] A. Hermant, "Optimal control of the atmospheric reentry of a space shuttle by an homotopy method," *Optimal Control Applications and Methods*, vol. 32, no. 6, pp. 627–646, 2011.

[27] A. Miele, Z. Zhao, and W. Lee, "Optimal trajectories for the aeroassisted flight experiment. part 1: Equations of motion in an earth-fixed system," Tech. Rep., 1989.

[28] J. D. Schierman, D. G. Ward, J. R. Hull, N. Gandhi, M. Oppenheimer, and D. B. Doman, "Integrated adaptive guidance and control for reentry vehicles with flight test results," *Journal of Guidance, Control, and Dynamics*, vol. 27, no. 6, pp. 975–988, 2004.

[29] E. Mooij, "The motion of a vehicle in a planetary atmosphere," *Delft University of Technology, Faculty of Aerospace Engineering, Report LR-768*, 1994.

[30] E. Musk, "Making life multi-planetary," *New Space*, vol. 6, no. 1, pp. 2–11, 2018.

[31] B. Tian and Q. Zong, "Optimal guidance for reentry vehicles based on indirect legendre pseudospectral method," *Acta Astronautica*, vol. 68, no. 7-8, pp. 1176–1184, 2011.

[32] J. L. H. Villar and J. P. V. S. da Cunha, "Controladores por modo deslizante para a umidade do solo modelado por equação diferencial parcial parabólica não-linear," in *Simpósio Brasileiro de Automação Inteligente-SBAI*, vol. 1, no. 1, 2021.